

Enhanced tunneling magnetoresistance in Fe/ZnSe double junctions: *Ab initio* calculations

J. Peralta-Ramos^{1,*} and A. M. Llois^{1,2}

¹*Departamento de Física, Centro Atómico Constituyentes, Comisión Nacional de Energía Atómica, Buenos Aires, Argentina*

²*Departamento de Física, Facultad de Ciencias Exactas y Naturales, Universidad de Buenos Aires, Buenos Aires, Argentina*

(Received 2 December 2005; revised manuscript received 31 March 2006; published 13 June 2006)

We calculate the tunneling magnetoresistance (TMR) of Fe/ZnSe/Fe/ZnSe/Fe (001) double magnetic tunnel junctions (DMTJs) as a function of the in-between Fe layer's thickness, and compare these results with those of Fe/ZnSe/Fe simple junctions. The electronic band structures are modeled by a parametrized tight-binding Hamiltonian fitted to *ab initio* calculations, and the conductance is calculated in the coherent, elastic and linear response regime within the Landauer formalism. We find that the DMTJs' TMR values can be higher than those of simple junctions, and that the TMR enhancements are mainly due to a decrease in the conductance of all but one spin channel and not due to the spin-dependent resonant tunneling effect. For a wide ZnSe width range, the TMR enhancements are large and practically independent of the in-between Fe thickness, which may be relevant for applications in spintronics.

DOI: [10.1103/PhysRevB.73.214422](https://doi.org/10.1103/PhysRevB.73.214422)

PACS number(s): 85.75.-d, 72.25.Mk, 73.23.Ad, 73.40.Rw

A magnetic tunnel junction (MTJ) consists of two ferromagnetic electrodes separated by a thin nonconducting barrier. It is experimentally observed that the conductance of a MTJ depends on the relative orientation of the electrodes' magnetization, and because of this, during the last years a lot of attention has been paid to the investigation of MTJs as promising candidates for their application in spintronic devices, such as read-heads and magnetic random access memories (see, for instance, Refs. 1 and 2, and references therein).

One of the challenges, that has to be overcome for practical applications, is to reach higher values of the tunneling magnetoresistance (TMR), defined as $TMR = [(\Gamma_P - \Gamma_{AP})/\Gamma_P] \times 100\%$, where Γ_P and Γ_{AP} are the conductances measured for the parallel (P) and antiparallel (AP) magnetization of the electrodes. Several possibilities are now being considered: to use highly polarized materials (*half-metals*) or dilute magnetic semiconductors as parts of MTJs to be able to inject spin-polarized currents into the semiconductor (see, for example, Refs. 3 and 4), to produce MTJs with almost perfect interfaces in order to favor the "symmetry enforced" spin-polarization of the current due to the barrier's complex band structure (see, for example, Ref. 5), and to make use of the so called *spin-dependent resonant tunneling effect* (SDRT) (Ref. 6) present in the coherent regime in epitaxial double magnetic tunnel junctions (DMTJs), in which a magnetic slab is inserted inside the semiconductor barrier of a simple MTJ. In this work we theoretically explore the latter alternative, namely, transport through DMTJs, and show that, at least for the Fe/ZnSe DMTJs studied here and with the approximations that we use, the TMR enhancements that we obtain with respect to simple MTJs originate *mainly* from a decrease in the conductance of all but one spin channel and not from the SDRT effect. We also show that, under certain conditions, the TMR enhancements that we obtain are practically independent of the midlayer's thickness.

The SDRT effect occurs in DMTJs because the quantum well states in the midlayer are spin split and can become, in certain cases, resonant states which can lead to very high

TMR values, as shown for the simple systems theoretically studied in Refs. 6–8. However, the experimental realization of the SDRT effect is difficult because interface roughness may either destroy the resonant levels or preclude the matching between the evanescent states in the barrier and the quantum well states in the midlayer. In spite of this, recent advances in growth techniques make it possible the observation of conductance and TMR oscillations as a function of both bias voltage and mid layer thickness, in fully epitaxial Fe/MgO/(Fe islands)|MgO/Fe (Ref. 9) and FM/NM/I/FM (Refs. 10 and 11) double junctions (FM: ferromagnet; NM: nonmagnetic metal; I: amorphous insulator), being the resonant tunneling effect mediated by quantum well states a possible explanation of these oscillations.^{9–12} Although it is nowadays possible to grow fully epitaxial double junctions, the main drawback of the use of the SDRT effect for applications is that it is very sensitive to the midlayer's thickness, which is very difficult to control experimentally.

Since Zhang *et al.*⁶ suggested using DMTJs as a way to achieve larger TMR values, several groups^{6,13–17} have theoretically shown that DMTJs exhibit richer spin-dependent transport properties than MTJs, especially with respect to the TMR dependence on the applied bias voltage, and that the TMR can be higher than that of MTJs due to the SDRT effect, but only recently could these epitaxial DMTJs be successfully fabricated.^{9,18,19} For example, Nozaki *et al.*¹⁹ have lately measured the TMR of fully epitaxial Fe/MgO (001) DMTJs with very clean and flat interfaces and in which the midlayer is an ordered Fe slab of 1.5 nm, and found (a) a moderate enhancement of the TMR with respect to MTJs at low bias and at room temperature, and (b) an extremely small bias voltage dependence of the TMR. These findings indicate that DMTJs may present advantages over MTJs for their use in spintronics, although more experiments on DMTJs are needed to confirm this assertion and to elucidate the origin of these features.

From the theoretical side, up to now the studies of DMTJs *with metallic magnetic layers in between the semiconductor* focused on the SDRT effect and were made within the free electron model (that cannot reproduce the decay rates of evanescent states).

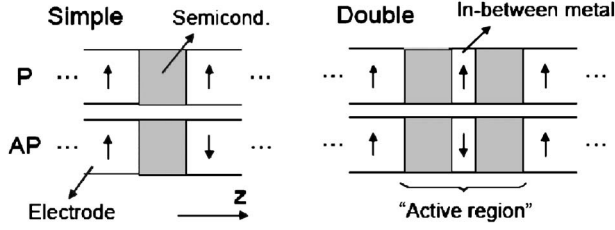


FIG. 1. Schematic structure of simple and double junctions, and magnetic configurations considered: parallel (P) and antiparallel (AP). The arrows indicate the magnetization direction in the metallic regions.

nescent states with different symmetries inside the semiconductor), and using rectangular potential profiles.^{6,13–15,17} Moreover, except for Ref. 15, these studies analyze the dependence of the TMR on the applied bias voltage and not on the in-between metallic layer’s thickness, as we do in this work. For this reason, in this paper *coherent* transport through $\text{Fe}(\infty)/\text{ZnSe}(a)/\text{Fe}(\infty)$ (001) MTJs and through $\text{Fe}(\infty)/\text{ZnSe}(b)/\text{Fe}(c)/\text{ZnSe}(b)/\text{Fe}(\infty)$ (001) DMTJs is theoretically investigated using a realistic tight-binding (TB) Hamiltonian in order to obtain the electronic structure of the junctions. $\text{Fe}(\infty)$ are semi-infinite electrodes, and a , b , and c denote thicknesses. The systems studied are epitaxial, and we restrict it to zero temperature, infinitesimal bias voltage, and elastic transport. We choose Fe/ZnSe because it can be grown epitaxially and because it shows very little interdiffusion at the interfaces, thus producing crystalline junctions in which there are no magnetically dead Fe layers.^{20,21} Moreover, in contrast to what happens in Fe/MgO based junctions, there is no oxidation of the interface Fe layers, which is known to be detrimental to TMR.²²

Figure 1 schematically shows the structure of simple and double junctions together with the different magnetic configurations considered, that is, parallel (P) and antiparallel (AP). Since the coercive fields of the electrodes and of the in-between Fe layers are different, the magnetic configurations shown are experimentally attainable.¹⁹ We call the “active region” of the junction (AR) to whatever is sandwiched by the electrodes. For the DMTJs, the AR consists of an “in-between metal region” (IBMR) sandwiched by two identical “semiconductor regions” (SCRs), while for the “corresponding” MTJs the AR is simply the SCR of the same width as each SCR of the DMTJs.

The conductances are calculated from the AR’s Green’s function $G_S^\sigma = [\hat{1}E - H_S^\sigma - \Sigma_L^\sigma - \Sigma_R^\sigma]^{-1}$, where $\hat{1}$ stands for the unit matrix, H_S^σ is the AR’s Hamiltonian, and $\Sigma_{L/R}^\sigma$ are the self-energies describing the interaction of the AR with the left (L) and right (R) electrodes (σ corresponds to the majority or minority spin channels). The energy E is actually $E_F + i\eta$, with E_F being the Fermi level of the system, and we take $\eta \rightarrow 0^+$. The self-energies are given by $\Sigma_L^\sigma = H_{LS}^\dagger g_{LS}^\sigma H_{LS}$ and $\Sigma_R^\sigma = H_{RS}^\dagger g_{RS}^\sigma H_{RS}$, where H_{LS} and H_{RS} describe the coupling of the AR with the electrodes, and $g_{L/R}^\sigma$ are the surface Green’s functions for each electrode. The surface Green’s functions are calculated using a semianalytical method²³ and are exact within our TB approximation. The transmission probabilities T^σ are given by²⁴ $T^\sigma(k_{||}, E_F) = \text{Tr}[\Delta_L^\sigma G_S^\sigma \Delta_R^\sigma G_S^{\sigma\dagger}]$

where $\Delta_{L/R}^\sigma = i(\Sigma_{L/R}^\sigma - \Sigma_{L/R}^{\sigma\dagger})$, while the conductances are given by $\Gamma^\sigma(E_F) = (e^2/hN_{k_{||}}) \sum_{k_{||}} T^\sigma(k_{||}, E_F)$, where $N_{k_{||}}$ is the total number of wave vectors parallel to the interface that we consider in our calculations. Since the junctions we study in this work are fully epitaxial, we assume that $k_{||}$ is conserved during electron tunneling, and since the IBMRs are thin (< 2.3 nm), we assume that spin is conserved as well.

As already mentioned, we restrict ourselves to the coherent regime, in which an electron coming from the left electrode tunnels to the right electrode through the entire active region conserving its phase. This is opposed to what happens in the sequential regime, in which the metallic midlayer acts as a floating gate to and from which electrons can tunnel losing their initial phase.^{15,24} In the latter regime, the DMTJs’ TMR values are lower or equal to those of the corresponding MTJs, while in the coherent regime the DMTJs’ TMR values can exceed those of the corresponding MTJs. In the coherent regime, the active region can be considered as a whole and electron transport can be described in terms of only one transmission probability T^σ for each spin, while in the sequential regime this is not possible and one must use two transmission probabilities for each spin: from the left electrode to the midlayer and from the midlayer to the right electrode. In reality, transport occurs through both mechanisms, but, at low temperatures, in fully epitaxial double junctions and in the absence of randomly spin oriented magnetic impurities, coherent tunneling is dominant.^{15,24}

Before discussing the three-dimensional (3D) Fe/ZnSe systems, we calculate the conductance of a *two-dimensional paramagnetic* double tunnel junction (2DDJ). Although the 2DDJs are not representative of real systems, they allow us to obtain some insight into resonant tunneling through double junctions, and show that, as already mentioned, a fine control of the IBMR thickness is essential to achieving resonant tunneling. The 2DDJs are of the type $M(\infty)/S/M/S/M(\infty)$, where $M(\infty)$ are semi-infinite paramagnetic metallic electrodes, S is a semiconductor, and M is a metal (the same as in the electrodes). In our model 2DDJs, the metal and the semiconductor have the same crystal structure, a *square* Bravais lattice with two atoms per unit cell, and are periodic in the direction perpendicular to the transport direction. The 2DDJs electronic structure is modeled by a second nearest neighbors TB Hamiltonian with one s orbital per atom, with the TB parameters chosen so as to make E_F fall in the middle of the semiconductor’s band gap (of 0.5 eV). The SCRs and IBMR thicknesses are varied between 1 and 10 layers. $N_{k_{||}} = 400$ is enough in this case to obtain convergence in the conductance.

We find that, for certain thicknesses of the IBMR, the conductance presents peaks in which it is enhanced from 1 to 4 orders of magnitude with respect to other IBMR widths. Figure 2 shows an example corresponding to 2DDJs with SCRs of four layers each. When the conductance is enhanced we always find, at certain values of $k_{||}$ (different for each IBMR thickness), resonant states at E_F that extend throughout the whole junction, and which are responsible for this enhancement. These resonant states move in energy when the IBMR thickness changes, and it is due to this that the conductance enhancement appears only for certain metal thick-

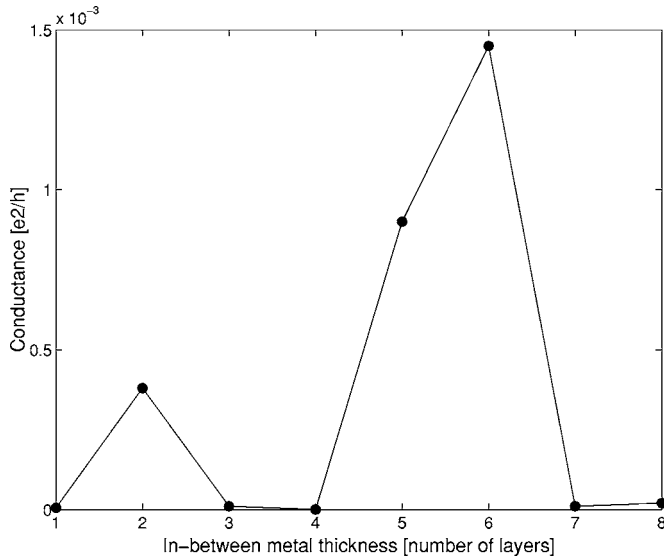


FIG. 2. Conductance as a function of in-between metal thickness for 2DDJs with semiconductor regions of four layers each.

nesses. At resonance, the 2DDJs conductances are slightly higher than the ones corresponding to simple 2D junctions, as it can be seen in Fig. 3. This figure shows the maximum obtainable ratio between the conductance of the 2DDJs and their corresponding 2D simple junctions as a function of the SCRs thickness. For SCRs thicknesses larger than four layers the enhancement effect is lost. This is because this thickness is very close to the decay length of the evanescent states inside the semiconductor (which can be obtained from its complex band structure) and so the IBMR quantum well states can no longer couple to these evanescent states to form resonances.

Having mentioned the main results obtained for resonant tunneling through 2DDJs, we undertake the discussion of the 3D $\text{Fe}(\infty)/\text{ZnSe}/\text{Fe}/\text{ZnSe}/\text{Fe}(\infty)$ (001) DMTJs. Figure 4

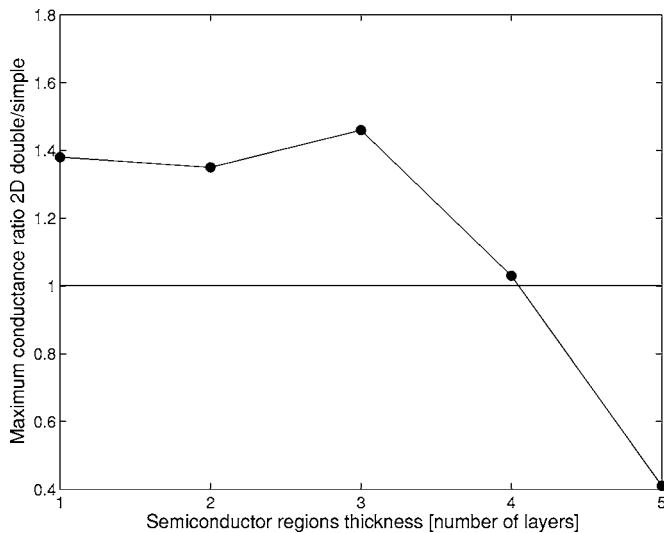


FIG. 3. Maximum ratio between the conductances of 2DDJs and simple 2D junctions as a function of the semiconductor regions thickness.

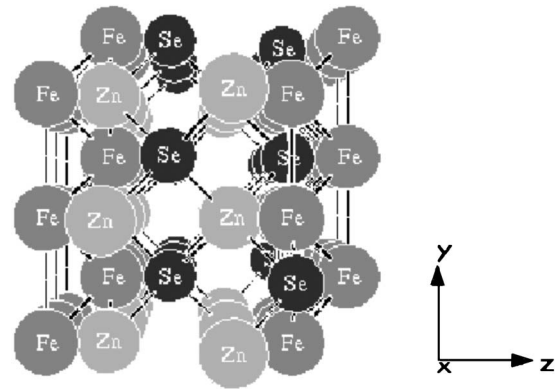


FIG. 4. Interface structure along the (001) direction of a Fe/ZnSe simple junction with a semiconductor's thickness of 5.67 \AA . The system is periodic in the x - y plane and the Fe electrodes are semi-infinite.

shows the structure of a simple $\text{Fe}(\infty)/\text{ZnSe}/\text{Fe}(\infty)$ junction with a SCR of 5.67 \AA , along the z direction (which is the direction of transport, see Fig. 1). The junctions are periodic in the x - y plane. The BCC Fe lattice parameter is 2.87 \AA , and that of zinc blende ZnSe is 5.67 \AA . The electronic structure of the junctions is modeled by a parametrized second nearest neighbors *spd* TB Hamiltonian fitted to *ab initio* calculations for both bulk Fe and bulk ZnSe.^{25,26} The hoppings between the Fe atoms and the (Zn,Se) atoms in the junctions are calculated using Shiba's rules and Andersen's scaling law.²⁷ The Fe *d* bands are spin split by μJ_{dd} , where $\mu = 2.2 \mu_B$ is the experimental magnetic moment of Fe and $J_{dd} = 1.16 \text{ eV}$ is the exchange integral between Fe *d* orbitals (μ_B is Bohr's magneton). With this value for μJ_{dd} , the bulk Fe *d* bands spin splitting is very well reproduced.²⁵ In our DMTJs, the Fe midlayer *d* bands splitting is the same as the one corresponding to bulk Fe. When forming the junctions, the ZnSe TB on-site energies are rigidly shifted to make the iron Fermi energy fall 1 eV above the ZnSe valence band and 1.1 eV below the conduction band, as indicated in photoemission experiments performed on Fe/ZnSe junctions.²⁰ We emphasize that, in our Fe/ZnSe DMTJs, the IBMR consists of an ordered ferromagnetic Fe slab with the same crystal structure as that of the electrodes (BCC) and with a thickness of at least two monolayers (2.87 \AA), and not a thin sheet of magnetic impurities of submonolayer thickness, in which case it has been shown, both theoretically and experimentally,²⁸ that the TMR values are notoriously lowered with respect to those of simple MTJs due to spin-flip processes and/or impurity assisted tunneling. These processes can also occur in DMTJs even when the IBMR is an ordered slab, but in this work we do not take them into account. In these 3D calculations, $N_{k_{ij}} = 5000$ is enough to achieve convergence in the conductances.

For simple junctions, we find that the conductances decay almost exponentially with semiconductor thickness with a different decay length for each spin channel (as expected from our complex bands calculations) and that the TMR increases and is always positive, reaching a value of 90% for a semiconductor thickness of 34 \AA . Our results are in very good agreement with the *ab initio* ones of Ref. 29.

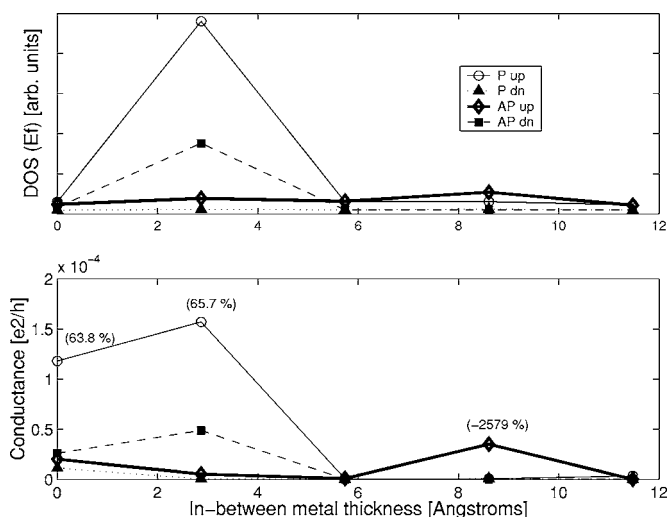


FIG. 5. Active region's density of states and conductances as a function of in-between metal thickness, for DMTJs with semiconductor regions of 22.7 Å each. The numbers in brackets shown in the lower panel are the corresponding TMR values.

For double junctions, we vary the SCRs thickness between 5.67 Å and 28.35 Å, and the IBMR thickness between 2.87 Å and 23 Å. As it happens in the 2DDJs, for certain width combinations of the SC and IBM regions the conductances can be higher than those of MTJs, in agreement with previous reports based on free electron models.^{6,13–15} Going over to the TMR values, we find that they can be enhanced due to a combination of: (i) an increase in the conductance of one particular spin channel due to the SDRT effect, as in Ref. 6, 8, 16, and 17; and (ii) a drop in the conductance of some spin channels due to the *spin-filter effect* (SFE). In our DMTJs, the TMR enhancements are mainly due to (ii), contrary to what has been reported in previous studies based on free electron models and rectangular potential profiles, that focus their attention on the SDRT effect. Both effects (i) and (ii) stem from a change in the active region's density of states (DOS) near E_F , induced by the presence of the in-between Fe layers, but are otherwise of a very different kind. In (i), transport occurs mainly through spin-split resonant levels that move in energy when the IBMR thickness changes (as discussed for the 2D example), while in (ii) an electron coming from the left electrode encounters a spin-dependent potential at the IBMR, and has a different transmission probability depending on its spin. The potential is spin-dependent because the mismatch between the electronic structure of the electrodes and that of the IBMR is different for each spin channel, as it happens, for instance, in the well-known case of Co/Cu multilayers.

As an example of resonance conductance enhancement in Fe/ZnSe DMTJs, we show in Fig. 5 the active region's total DOS at E_F for each spin channel, as a function of the IBMR thickness for DMTJs with the SCR widths of 22.7 Å each, together with the corresponding conductances. An increase in the DOS of one order of magnitude takes place for an IBMR of 2.87 Å in the P majority channel and in the AP minority channel, and a smaller increase appears for an IBMR of 8.6 Å in the AP majority channel. The DOS peaks

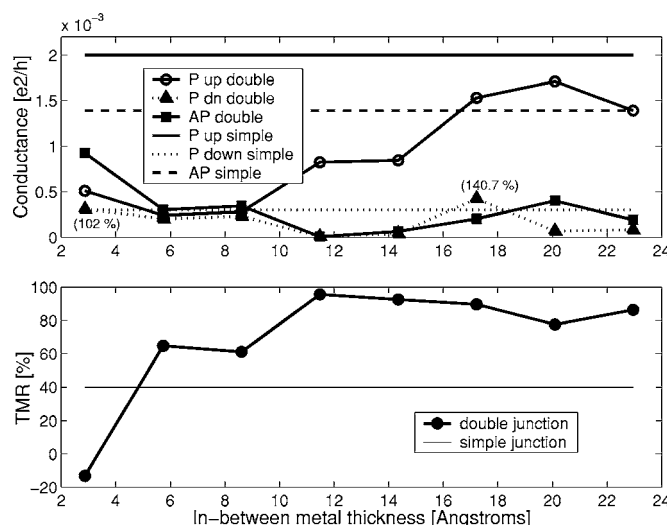


FIG. 6. Conductance and TMR values of DMTJs with SCRs of 17 Å, and those of the corresponding simple junction, as a function of the in-between metal thickness. The numbers in brackets are the ratios between the DMTJs and MTJs conductances, $\times 100$.

coincide with a conductance enhancement in the mentioned three channels of 1–3 orders of magnitude with respect to other IBMR thicknesses, showing that the origin of this enhancement is the same as that discussed for 2DDJs, namely, resonant tunneling. When there is a conductance enhancement, we find that as a function of the energy the conductance is sharply peaked at E_F , confirming that this increase is due to resonant states and not to the SFE, in which cases we obtain that the conductances are smooth functions of the energy (since the potential does not change abruptly with the energy). Figure 5 also shows that for an IBMR width of 2.87 Å, the resonances in the P majority and the AP minority channels compete with each other and this results in a TMR value (shown in brackets in the lower panel) very close to that of the corresponding MTJ (65.7% vs 63.8%). In contrast, for an IBMR of 8.6 Å the TMR becomes very large and negative due to the AP majority resonance.

By varying the IBMR width for all the SCRs' thicknesses considered, we obtain that for SCRs with thicknesses below 23 Å the Fe/ZnSe DMTJs' TMR values can be 2–3 times higher than those of the corresponding MTJs, while the conductance of some spin channels remain of the same order of magnitude or larger (so that their measurement is possible). For this SCRs width range, the TMR enhancement is mainly due to (ii), one exception being the resonance in the AP channel for an IBMR thickness of 8.6 Å, shown in Fig. 5. Beyond this SCRs' thickness (23 Å), the conductances of all the spin channels are 4–6 orders of magnitude smaller than the corresponding MTJs values, thus becoming hard to measure and of little physical interest.

To visualize the interplay among the conductance values of the different channels and configurations and their contribution to the TMR in the SCRs width range of interest, we show in Fig. 6, as an example, the conductances and TMR values as a function of IBMR thickness for Fe/ZnSe DMTJs with SCRs of 17 Å. It is seen that for Fe widths larger than 6 Å the TMR is 1.5–2 times higher than that of the simple

MTJ, and that the TMR values are enhanced mainly due to (ii). For IBMR thicknesses larger than 10 Å, the IBMR is almost transparent for the P majority electrons, while the conductances of the other spin channels are considerably quenched, which results in large and positive TMR values. For very thin Fe mid layers the TMR obtained for these DMTJs is negative and rather low, and for IBMR thicknesses in the range 12–23 Å the TMR values are high and almost constant. This behavior is similar to the one obtained for other SCRs widths smaller than 23 Å, and shows that a mid-layer width range exists (12–23 Å) for which a *fine control of the IBMR thickness is not critical to achieve significant TMR enhancements*, something that may be relevant for applications. However, this fine control is indispensable for tuning conductance resonances, which can lead, as already shown, even to an inversion of the TMR (see Fig. 5). The fact that to achieve TMR enhancements it is not necessary to finely control the IBMR thickness is, for us, the most important result of this work. It shows that the SDRT effect (difficult to control in practice due to the already mentioned reasons) is not essential for these TMR enhancements to occur.

In summary, based on realistic electronic structure and accurate conductance calculations, we predict large TMR enhancements for fully epitaxial Fe/ZnSe double magnetic tun-

nel junctions with respect to Fe/ZnSe simple junctions, in the coherent, elastic, and linear response regime. The enhancements are mainly due to a decrease in the conductance of all but one spin channel and not to spin-dependent resonant tunneling, and for a wide ZnSe width range they are practically independent of the Fe midlayer thickness.

We should mention that the presence of interface roughness, defects, and impurities in the DMTJs may reduce the enhancements obtained in our calculations, leading even to a suppression of the TMR effect due to spin-flip scattering and/or impurity assisted tunneling.²⁸ Further theoretical investigations of transport through double magnetic tunnel junctions relying on realistic electronic structure calculations and including finite bias voltage, temperature effects, and inelastic processes, as well as the measurement of the TMR as a function of the midlayer thickness and bias voltage, are highly desirable to improve our understanding of these scarcely studied systems, which may be useful in the design of future spintronic devices.

We are grateful to Julián Milano for useful discussions. This work was partially funded by UBACyT-X115, Fundación Antorchas, PICT 03-10698, and PIP-Conicet 6016. Ana María Llois belongs to CONICET (Argentina).

*Author to whom correspondence should be addressed. Electronic address: peralta@cnea.gov.ar

¹E. Y. Tsybal, O. N. Mryasov, and P. R. LeClair, *J. Phys.: Condens. Matter* **15**, 109 (2003).

²I. Zutic, J. Fabian, and S. Das Sarma, *Rev. Mod. Phys.* **76**, 323 (2004).

³A. M. Bratkovsky, *Appl. Phys. Lett.* **72**, 2334 (1998); M. Bowen, M. Bibes, A. Barthélémy, J.-P. Contour, A. Anane, Y. Lemaitre, and A. Fert, *ibid.* **82**, 233 (2003); Z. Sefrioui, V. Cros, A. Barthélémy, V. Peña, C. León, J. Santamaría, M. Varela, and S. J. Pennycook, *ibid.* **88**, 022512 (2006).

⁴M. Tanaka and Y. Higo, *Phys. Rev. Lett.* **87**, 026602 (2001); D. Chiba, F. Matsukura, and H. Ohno, *Physica E (Amsterdam)* **21**, 966 (2004); V. Garcia, H. Jaffres, M. Eddrief, M. Marangolo, V. H. Etgens, and J.-M. George, *Phys. Rev. B* **72**, 081303(R) (2005).

⁵S. Yuasa, T. Katayama, T. Nagahama, A. Fukushima, H. Kubota, Y. Suzuki, and K. Ando, *Appl. Phys. Lett.*, **87** 222508 (2005); J. P. Velev, K. D. Belashchenko, D. A. Stewart, M. van Schilf-gaarde, S. S. Jaswal, and E. Y. Tsybal, *Phys. Rev. Lett.* **95**, 216601 (2005).

⁶X. Zhang, B.-Z. Li, G. Sun, and F.-C. Pu, *Phys. Rev. B* **56**, 5484 (1997).

⁷F. Giazotto, F. Taddei, R. Fazio, and F. Beltram, *Appl. Phys. Lett.* **82**, 2449 (2003).

⁸A. G. Petukhov, A. N. Chantis, and D. O. Demchenko, *Phys. Rev. Lett.* **89**, 107205 (2002).

⁹T. Nozaki, N. Tezuka, and K. Inomata, *Phys. Rev. Lett.* **96**, 027208 (2006).

¹⁰S. Yuasa, T. Nagahama, T. Kawakami, K. Ando, and Y. Suzuki, *J.*

Phys. D **35**, 2427 (2002).

¹¹T. Nozaki, Y. Jiang, Y. Kaneko, A. Hirohata, N. Tezuka, S. Sugimoto, and K. Inomata, *Phys. Rev. B* **70**, 172401 (2004).

¹²J. Mathon and A. Umerski, *Phys. Rev. B* **71**, 220402(R) (2005); Z. Y. Lu, X. G. Zhang, and S. T. Pantelides, *Phys. Rev. Lett.* **94**, 207210 (2005).

¹³L. Sheng, Y. Chen, H. Y. Teng, and C. S. Ting, *Phys. Rev. B* **59**, 480 (1999).

¹⁴B. Wang, Y. Guo, and B.-L. Gu, *J. Appl. Phys.* **91**, 1318 (2002).

¹⁵Z. P. Niu, Z. B. Feng, J. Yang, and D. Y. Xing, *Phys. Rev. B* **73**, 014432 (2006).

¹⁶Y.-M. Zhang and S.-J. Xiong, *Physica B* **362**, 29 (2005).

¹⁷Z. Zheng, Y. Qi, D. Y. Xing, and J. Dong, *Phys. Rev. B* **59**, 14505 (1999); Z. Y. Zeng, B. Li, and F. Claro, *ibid.* **68**, 115319 (2003).

¹⁸Z.-M. Zeng, X.-F. Han, W.-S. Zhan, Y. Wang, Z. Zhang, and S. Zhang, *Phys. Rev. B* **72**, 054419 (2005); J. H. Lee, K.-I. Jun, K.-H. Shin, S. Y. Park, J. K. Hong, K. Rhie, and B. C. Lee, *J. Magn. Magn. Mater.* **286**, 138 (2005).

¹⁹T. Nozaki, A. Hirohata, N. Tezuka, S. Sugimoto, and K. Inomata, *Appl. Phys. Lett.* **86**, 082501 (2005).

²⁰M. Eddrief, M. Marangolo, S. Corlevi, G.-M. Guichar, V. H. Etgens, R. Mattana, D. H. Mosca, and F. Sirotti, *Appl. Phys. Lett.* **81**, 4553 (2002).

²¹M. Marangolo, F. Gustavsson, M. Eddrief, Ph. Sainctavit, V. H. Etgens, V. Cros, F. Petroff, J. M. George, P. Bencok, and N. B. Brookes, *Phys. Rev. Lett.* **88**, 217202-1 (2002).

²²X.-G. Zhang, W. H. Butler, and A. Bandyopadhyay, *Phys. Rev. B* **68**, 092402 (2003).

²³S. Sanvito, C. J. Lambert, J. H. Jefferson, and A. M. Bratkovsky, *Phys. Rev. B* **59**, 11936 (1999).

- ²⁴S. Datta, *Electronic Transport in Mesoscopic Systems* (Cambridge University Press, Cambridge, 1999).
- ²⁵D. A. Papaconstantopoulos, *Handbook of the Band Structure of Elemental Solids* (Plenum, New York, 1986).
- ²⁶R. Viswanatha, S. Sapra, B. Satpati, P. V. Satyam, B. N. Dev, and D. D. Sarma, cond-mat/0505451, Phys. Rev. B. (to be published).
- ²⁷O. K. Andersen, Physica B **91**, 317 (1977); J. Mathon, Phys. Rev. B **56**, 11810 (1997).
- ²⁸A. M. Bratkovsky, Phys. Rev. B **56**, 2344 (1997); R. Jansen and J. C. Lodder, *ibid.* **61**, 5860 (2000); R. Jansen and J. S. Moodera, *ibid.* **61**, 9047 (2000).
- ²⁹J. M. MacLaren, X.-G. Zhang, W. H. Butler, and X. Wang, Phys. Rev. B **59**, 5470 (1999).